# New engineering science insights into the electrodes pairing of electrochemical energy storage devices assisted by machine learning

**Longbing Qu**
The University of Melbourne
**Peiyao Wang**
University of Melbourne
**Benyamin Motevalli**
The University of Melbourne
**Qinghua Liang**
The University of Melbourne https://orcid.org/0000-0001-5980-9371
**Kangyan Wang**
The University of Melbourne
**Wen-Jie Jiang**
The University of Melbourne
**Jefferson Zhe Liu**
University of Melbourne https://orcid.org/0000-0002-5282-7945
**Dan Li** ( dan.li1@unimelb.edu.au )
The University of Melbourne https://orcid.org/0000-0003-3461-5751

**Article**

**Keywords:**

**Posted Date:** May 18th, 2022

**DOI:** https://doi.org/10.21203/rs.3.rs-831006/v1

# New engineering science insights into the electrodes pairing of electrochemical energy storage devices assisted by machine learning

Longbing Qu[1,2], Peiyao Wang[1,2], Benyamin Motevalli[1], Qinghua Liang[2], Kangyan Wang[2], Wen-Jie Jiang[2], Jefferson Zhe. Liu[1*] and Dan Li[2*]

[1]Department of Mechanical Engineering, The University of Melbourne, Melbourne, Victoria, Australia; [2]Department of Chemical Engineering, The University of Melbourne, Melbourne, Victoria, Australia.; Corresponding author Email: dan.li1@unimelb.edu.au (D.L.); zhe.liu@unimelb.edu.au (J.Z.L.)

**Pairing the positive and negative electrodes with their individual dynamic characteristics properly matched is essential to the optimal design of electrochemical energy storage devices. However, the complex relationship between the performance data measured for individual electrodes and the two-electrode cells used in practice often makes an optimal pairing experimentally challenging. In this work, taking graphene-based supercapacitors as an example, we combine experiments with machine learning to generate a large pool of capacitance data for graphene-based electrode materials with varied slit pore sizes and thicknesses, and numerically pair them into different combinations for two-electrode cells. The as-achieved pairing results allow us to conduct a comprehensive analysis of the correlations between the key electrode structural features of individual electrodes and volumetric capacitance of the resultant two-electrode cells. The results show that the optimal pairing parameters are varied considerably with the operation rate of the cells and are even influenced by the thickness of the inactive components. The best-performing individual electrode does not necessarily result in optimal cell-level performance. The machine learning-assisted pairing approach presents much higher efficiency compared with the traditional trial-and-error approach for the optimal design of supercapacitors and provides an additional effective avenue for further improving the performance of supercapacitors and is expected to play an enabling role in the future on-demand design of energy storage devices. The results observed in this work also indicate the call for comprehensive performance data reporting in the electrochemical energy storage field to enable the adoption of artificial intelligence techniques to accelerate the translation of academic research in this rapidly growing field.**

Electrochemical energy storage devices (EESDs) such as batteries and supercapacitors play a critical enabling role in the realisation of a sustainable society[1]. A practical EESD is a multi-component system that consists of at least two active electrodes and other supporting materials such as separator and current collector. Understanding and optimising the interplays of individual components is essential to maximising the materials utilisation efficiency of the entire cell[2-4]. However, it has been a great challenge to quantitatively investigate the complex relationships between the individual components and the cell- or system-level performance[2,5]. Matching of different components such as the pairing of positive and negative electrodes in EESDs to achieve an optimal cell-level performance has so far largely relied on the conventional trial-and-error approach. The community, particularly from the industry side, calls for an engineering science approach that focuses on scientific method as a rigorous basis to develop optimised solutions for this challenging task through enhanced understanding and integrated application of mathematical, scientific, statistical, and engineering principles.

Taking supercapacitor as an example for EESDs and as to be reiterated below, how the two electrodes of supercapacitors are optimally paired plays a considerable role in the optimisation of the cell-level performance. The complex relationship between the structure of individual electrodes and the two-electrode cells makes it practically challenging to predict and optimise the electrodes pairing based on the performance data of individual electrodes[2,4,6]. Previous reports have demonstrated that the balancing of electrode mass[7], pore structure[8,9], charging rate[10,11], and working potential windows[12,13] can affect the performance of the as-paired supercapacitor cells. However, the electrodes pairing for supercapacitor cells have been generally carried out on the basis of a simplified performance relationship between individual electrodes and the two-electrode cells or through a limited number of experiments screening[6,7,14,15]. The past decades have seen tremendous progress in improving the energy storage capacity of supercapacitors through the discovery of new electrode materials[6,16,17] and electrolytes[18,19] and the improved understanding of the charging dynamics in nanoporous electrodes[20-24]. However, there have been few methods reported to quantitatively evaluate how the structural parameters of individual electrodes affect the capacitance of supercapacitor cells and whether a pairing reaches the optimum at various operating conditions of the supercapacitor cells. The lack of an effective strategy for electrode pairing thus presents a bottleneck to limit the full potential of high-performance individual electrode materials to be translated into a real supercapacitor device.

In the past few years, data science techniques, particularly machine learning (ML), have been introduced into the energy storage field to solve some challenging research questions of EESDs[25-29]. In battery research, ML has been applied for electrode material design, synthesis/manufacturing, and characterisation[30,31,32,33,34,35] as well as battery cell diagnosis and prognosis[36,37]. For supercapacitors, ML has been introduced for active material performance prediction and electrode optimal design[38-41]. These results clearly demonstrate the merit (high efficiency and cost effective) of combining experiment and data driven approach to address the complex energy material processing-structure-property relationship or device managements. It is promising to combine experiments and ML to investigate the complicated component-device relation to gain much-needed engineering science insights to accelerate the translation of breakthrough energy materials to cell-level performance under various working conditions.

In this work, we use graphene-based supercapacitors as a model system to analyse the complexity and necessity of a rational approach for electrodes pairing to optimise the performance of EESDs and demonstrate how the emerging ML and data science techniques can provide an effective solution to this long-standing problem. Briefly, we will first revisit the basic principles and key considerations of electrodes pairing for supercapacitors and discuss the need of a large performance data pool of individual electrodes under varied conditions for an optimal pairing. We then present a combined approach of experiments and ML to address this need. On the basis of a comprehensive analysis of the relationships between the electrode structures and the volumetric performance of the paired combinations, we highlight some new engineering science insights that are often overlooked yet important in the existing electrodes pairing practice. We conclude this article with a perspective on the enabling role of ML in the future on-demand design of EESDs.

**Revisit the principles of electrodes pairing engineering for supercapacitors**

As with other electrochemical devices, a supercapacitor cell in practical use must contain at least two electrodes connected in series, which are respectively charged positively and negatively during the charging process[7]. Assuming that no other side reactions or energy loss occur during the operation, the charges stored in the cell and both electrodes will be equal ($\Delta Q_{cell} = |\Delta Q_+| = |\Delta Q_-|$) at any time to ensure the charge balance between the two electrodes[42]. Because the positive and negative electrodes are connected in series in the cell, the working voltage of the cell will be a sum of the absolute values of working potential windows for the two electrodes ($\Delta U_{cell} = |\Delta U_+| + |\Delta U_-|$). Thus, the following relationships should be satisfied in the design of a supercapacitor[43]:

$$C_+ \times |\Delta U_+| = C_- \times |\Delta U_-| = C_{v+} \times V_+ \times |\Delta U_+| = C_{v-} \times V_- \times |\Delta U_-| \quad (1)$$

$$C_{cell} = (C_+ \times C_-)/(C_+ + C_-) \quad (2)$$

where $C_+$ and $C_-$ ($V_+$ and $V_-$) are the total capacitance (the corresponding electrode volume) for the individual positive and negative electrodes, respectively. $C_{v+}$ and $C_{v-}$ are volumetric capacitance of the corresponding electrodes against their volume. $\Delta U_+$ and $\Delta U_-$ are the working potential windows of positive and negative electrodes, respectively. $C_{cell}$ is the total capacitance of the supercapacitor cell.

It is worth pointing out that other engineering issues, often overlooked in the scientific literature, need to be considered in the design of EESDs. Apart from the electrodes that actively store energy, other supporting components such as the current collector, separator, and packaging materials are needed. These components are inactive for energy storage, but they take up a considerable amount of mass/volume of the cell, affecting the overall energy density of the whole cell[2,4]. To allow a reliable evaluation of the performance of a supercapacitor cell that is aligned with the requirement by the energy storage industry, the mass or volume of the entire device, including inactive components, needs to be considered[2,4]. The volumetric capacitance and energy density of the supercapacitor cells can thus be described as below[4,15]:

$$C_{v-cell} = C_{cell}/(V_+ + V_- + V_{inactive}) \quad (3)$$

$$E_{v-cell} = \frac{1}{2} C_{v-cell} \times \Delta U_{cell}^2 = \frac{1}{2} C_{v-cell} \times (|\Delta U_+| + |\Delta U_-|)^2 \quad (4)$$

where $C_{v-cell}$, $E_{v-cell}$, and $\Delta U_{cell}$ are the volumetric capacitance, energy density, and working voltage of a supercapacitor cell, respectively. $V_{inactive}$ refers to the volume of the inactive components. These equations indicate that the performance of a supercapacitor cell follows a nonlinear relationship with the capacitance of individual electrodes and the volume of inactive components.

More complicating for the supercapacitor design is that the two electrodes can involve different charging kinetics, particularly for asymmetric supercapacitors. Even for the same electrode materials, $C_{v+}$ and $C_{v-}$ can be different or exhibit different variation profiles against the operation rate[13,44,45]. The discrepancy between $C_{v+}$ and $C_{v-}$ is particularly remarkable when the $\Delta U_+$ and $\Delta U_-$ are adjusted to maximise the cell voltage ($\Delta U_{cell}$) to achieve the maximal $E_{v-cell}$ (Eq. 4)[13,14]. According to Eq. 1, a change in the ratio of $C_{v+}$ to $C_{v-}$ need to be compensated by the ratio of the electrode volume or the working voltage distribution of positive and negative electrodes in the cell. The variations of either $\Delta U_+(\Delta U_-)$ or $C_{v+}$ ($C_{v-}$) would then

affect the cell-level energy density (Eq. 4). Thus, it is a challenge to achieve the optimal electrode pairing parameters of the supercapacitors under various operating conditions using the experimental trial-and-error approach. Until now, the electrodes pairing for supercapacitors in the literature is generally carried out with simplified assumptions, for example, neglecting the divergence of charging kinetics in two pairing electrodes, the effect of inactive components, or the operation rate. As a result, the capacity of individual electrode materials in a supercapacitor cell is often underutilized.

As the volumetric capacitance of an individual electrode is dependent on several structural parameters such as the electrode thickness ($t$), pore size ($d$), and operating conditions such as working potential window and operation rate ($v$)[6,46,47], optimally pairing two electrodes at various operation conditions according to Eq. 1 will require a large number of electrochemical data of individual electrodes under various conditions. If all the data were to be obtained by experiments, it would be practically infeasible. Here, we will combine experiments with ML to build a predictive ML model to correlate the electrochemical performance of individual electrodes with the corresponding electrode structural features and operation rates. We will use the as-obtained model to generate the performance data of positive and negative electrodes for any given conditions and then numerically pair them into supercapacitor cells that meet Eq. 1 and calculate the volumetric capacitance of the cells based on Eqs. 2 and 3. To test the validity of the numerical paired results, we fabricated supercapacitor cells with the predictive paired structural parameters to evaluate the numerically paired results. The results have allowed us to analyse how the electrodes pairing affects the cell-level performance and establish the quantitative relationship of each structural/operation parameter for each electrode with the performance of the resultant two-electrode cell.

**Acquiring experimental capacitance database for individual electrodes**

Acquisition of a sufficient number of data is essential for training a reliable ML model. It has been widely documented in the literature that the pore size[48-50], thickness[2,4,15], and operation rates[6,10,11] are the primary parameters affecting the electrochemical perform ance of supercapacitors. ML has been recently used to predict the specific capacitance of activated porous carbon from the data collected from the literature[38-40]. However, given that the literature data were acquired from varied conditions and material sources and thus are unsuited for this work, we decided to obtain the experimental data from our own experiments by taking advantage of the broad-range structural tuneability of the multilayered reduced graphene oxide membranes (MGMs) we previously developed[6]. To achieve this, we first fabricated these

graphene-based electrodes with various slit pore sizes and thicknesses (see the details in **Supplementary Note 1** and **Supplementary Table 1**). We followed the previous practice[12,14,51] to maximise the cell voltage ($\Delta U_{cell}$) by respectively adjusting the working potential window of the positive and negative electrodes to be 0.55 and 1.05 V in an aqueous electrolyte of 1.0 M KCl (see the details in **Supplementary Note 2 and Supplementary Fig. 1-3**). Then, we obtained the volumetric capacitance of positive and negative electrodes under the intended working potential windows using the three-electrode electrochemical setup. The as-obtained experimental data were then used for ML to understand how the electrode polarization, pore size, and thickness collectively affect the electrochemical performance under various charging conditions at both individual electrodes and cell levels. The size of experimental data for fitting the ML models for either positive or negative electrodes is 100.

**Figure 1** presents the representative volumetric capacitance of the graphene-based electrodes with various pore sizes and thicknesses obtained from the three-electrode setup under a range of operation rates. The results show that the volumetric capacitance ($C_{v+}$ and $C_{v-}$) of the same graphene-based electrodes measured at the positive and negative potential windows give rise to rather different values. For example, at the tested operation rates, the value of $C_{v+}$ is always lower than that of $C_{v-}$. Such a variation has also been observed in activated porous carbon[52]. Both $C_{v+}$ and $C_{v-}$ show a nonlinear dependence on the slit pore size, thickness, and operation rates of electrodes (**Fig. 1**). For example, with the increase of the operation rate, there is an increase in the nonlinear relationship between volumetric capacitance and structural parameters of electrodes (**Supplementary Fig. 4**). Increasing the slit pore size of the electrode (**Fig. 1a**), the electrode thickness (**Fig. 1b**), or the charging rate (**Fig. 1c**) leads to reduced volumetric capacitance. These trends are consistent with the literature[6,15,46,49]. Although the trends can be qualitatively explained by the ion transport theories for porous electrodes, no theoretical models are available to explain and predict the results in a quantifiable manner due to the complex charging dynamics in nanopores[21,53,54]. The complex interplay of these parameters makes it even more challenging to quantify and predict the relationship between these parameters and the volumetric capacitance.

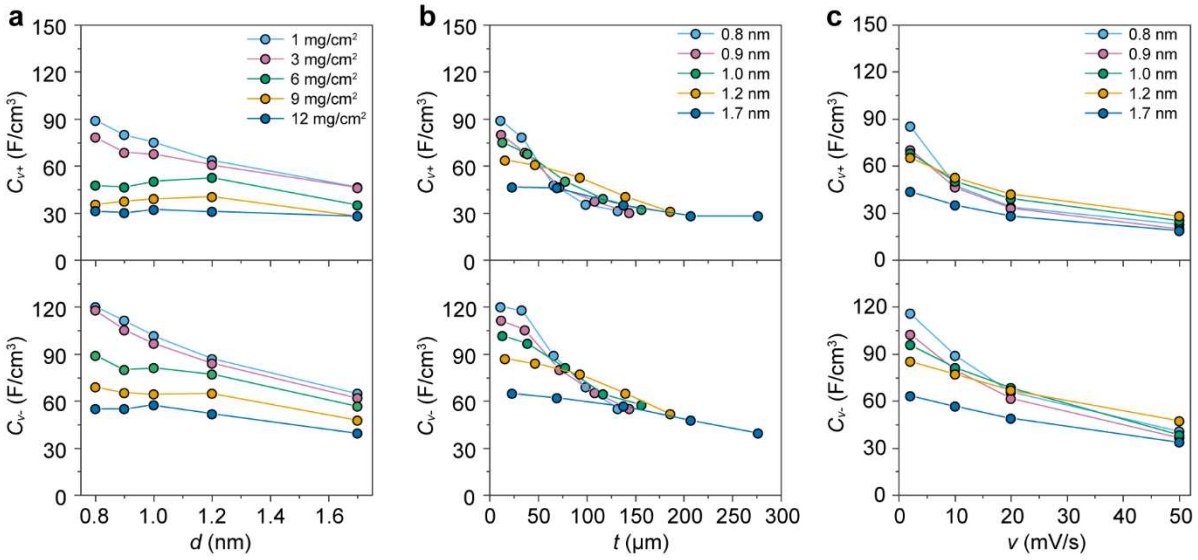


**Fig. 1 | Representative volumetric capacitance of the individual electrodes of graphene-based supercapacitors experimentally obtained under various conditions. a**, $C_{v+}$ (top) and $C_{v-}$(bottom) *vs*. the average slit pore size ($d$) of the graphene-based electrodes with varying areal mass loading. Only the data obtained at ν = 10 mV/s are presented in the plots. **b**, $C_{v+}$ (top) and $C_{v-}$(bottom) *vs*. the thickness ($t$) of the graphene-based electrodes with varying average slit pore size. Only the data obtained at ν = 10 mV/s are presented in the plots. **c**, $C_{v+}$ (top) and $C_{v-}$(bottom) *vs*. the charging rate ($v$) of the graphene-based electrodes. The data obtained with the electrode mass loading of 6 mg/cm$^2$ are plotted in this figure.

## Machine learning-assisted prediction of the volumetric capacitance of individual electrodes

After obtaining the experimental datasets of volumetric capacitance and corresponding structural parameters at different operating rates, we tested several kinds of ML algorithms including ridge regression, polynomial regression, random forest regression and artificial neural network (ANN). After analysing the results of these tested ML algorithms (**Supplementary Table 2**), we decided to use the ANN model to establish quantifiable relationships regarding how the key structural parameters of individual electrodes and the operation rate affect the volumetric performance of individual electrodes. The input descriptors of our ANN models include the electrode thickness and interlayer distance (or slit pore size) of electrode and operation (or charging) rate. The output is the volumetric capacitance of positive or negative electrodes. The middle part of the ANN structure is the hidden layers. The layers among the input layer, hidden layers, and output layer are connected by the weights (see the details in **Supplementary Note 3** and **Supplementary Fig. 5a**).

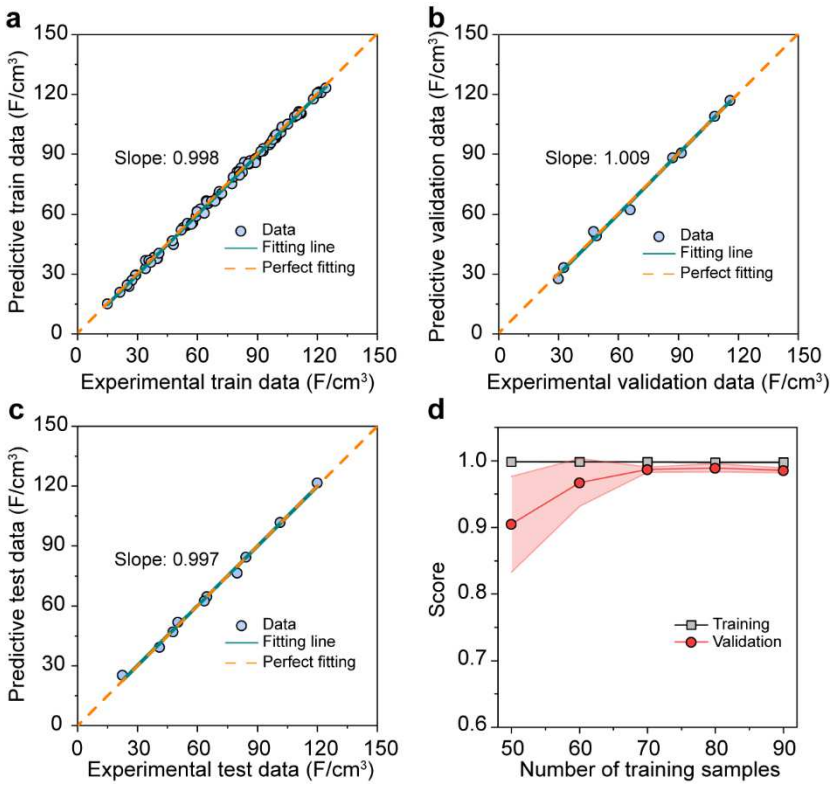


**Fig. 2 | Representative results of ANN model for the negative electrode**. **a**, **b,** and **c**, Model training results *vs.* experimental data, model validation results *vs.* experimental data, and model test results *vs.* experimental data of ANN model for the negative electrode, respectively. **d**, The cross-validation learning curve of the built ANN model for the negative electrode.

We allocated 80%, 10%, and 10% experimental datasets for training, validation, and test, respectively (**Supplementary Fig. 6**). We did the hyperparameters optimisation to select the suitable ANN network structure and learning rate (see the details in **supplementary file of hyperparameter, Supplementary Note 3** and **Supplementary Fig. 7**). After that, we conducted the ANN training (**Fig. 2a** and **Supplementary Fig. 5b**). To evaluate the trained ANN models, we compared the validation results and experimental data after the validation procedure. The validation analysis shows that the prediction results from the trained ANN models are in good agreement with the experimental data of positive and negative electrodes (both with the fitting slopes of 1.009) and with mean squared error (MSE) of 0.063% and 0.017%, respectively (**Supplementary Fig. 5c** and **Fig. 2b**). The reliability testing with the unseen data that was not used for the ML model training and validation process gives a fitting slope of 1.040 (positive electrode ANN model) and 0.997 (negative electrode ANN model) for experiment and prediction data (**Supplementary Fig. 5d** and **Fig. 2c**). The corresponding MSE for positive and negative models are 0.058% and 0.023%, respectively.

We also undertook the stratified shuffle split cross-validation approach to examine the reliability and sufficiency of the collected experimental data for the ANN models (**Supplementary Fig. 5e** and **Fig. 2d**). Generally, increasing the number of training examples results in a higher validation score and lower score variation. For example, when the number of the training sample reaches 80, the cross-validation score approaches 99%, with a score variation of 0.6%, suggesting the number of training samples used in our work is rather sufficient for the ANN model training to achieve a reasonably reliable ANN model, which is likely due to the high quality of the experimental data obtained from our well-controlled experiments and the appropriate choice of the key feature descriptors guided by the domain knowledge[55].

We then simulated 50,000 volumetric capacitance values predicted from the trained ANN models and plotted the results in the predictive 3D graphs shown in **Fig. 3**. All experimental data are located on the surface of the 3D graphs, further demonstrating the reliability of the as-obtained ANN models and the high accuracy of the predicted results. The nonlinear relationships indicated from these graphs also suggest the intertwined influence of the slit pore size, thickness, and operating rate of electrodes, indicating the challenge of obtaining a universal mathematical equation to predict the volumetric capacitance of the electrode materials using the traditional methods.

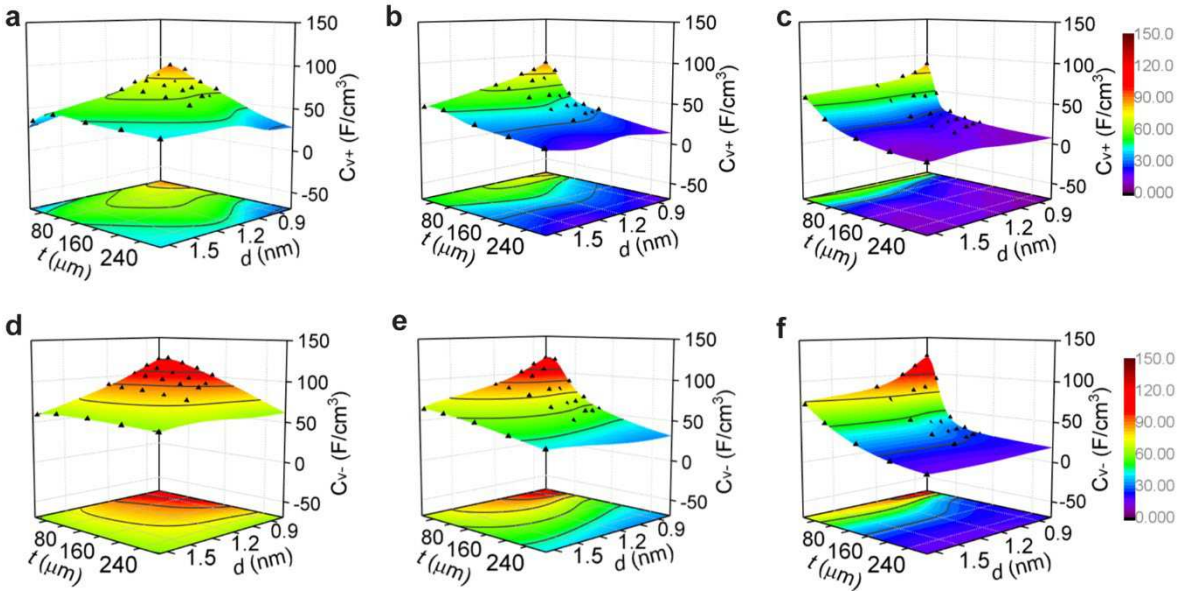


**Fig. 3 | Volumetric capacitance prediction of the graphene-based individual electrodes from the resulting ANN models**. **a-c,** The 3D surface and corresponding 2D projection figures (volumetric capacitance *vs.* slit pore size and thickness) under the scan rates of 2, 10, and 50 mV/s for the positive electrodes, respectively. **d-f,** The 3D surface figures and corresponding 2D projection figures

(volumetric capacitance *vs.* slit pore size and thickness) under the scan rates of 2, 10, and 50 mV/s for the negative electrodes, respectively; The triangles in black located at the surface of the 3D figures are the corresponding experimental data.

**Numerical pairing of electrodes and experimental testing**

To pair the positive and negative electrodes for a completed supercapacitor cell, we first generated an extensive dataset of the values for $C_{v+}$ and $C_{v-}$ under a given condition of electrode structural parameters (slit pore size ($d$) and electrode thickness ($t$)) and operation rate ($v$), with $d$ varied from 0.8 to 1.7 nm at an interval of 0.009 nm, $t$ varied from 11 to 276 μm at an interval of 0.53 μm, and $v$ varied from 2 to 50 mV/s, respectively. We thus obtained 50,000 volumetric capacitances of positive and negative electrodes for each under different operating rates. As a demonstration, we numerically paired the electrodes by satisfying Eq. 1 and calculated the volumetric capacitance based on Eqs. 2 and 3 for the cells working at 6, 30, and 75 mV/s, respectively, which resulted in 8,533,144, 5,320,777, and 3,576,000 paired combinations, respectively (see the details in **Supplementary Note 4** and **Supplementary Fig. 8**).

To further test the validity of our model and the numerical paired results, we conducted experiments to test whether the numerically paired results based on the predictive datasets can be reproduced by experiments. As a demonstration, we fabricated supercapacitor cells with the paired structural parameters (slit pore size and thickness) that were predicted to generate optimal volumetric capacitance values of 12.4 F/cm$^3$ at 6 mV/s, 9.1 F/cm$^3$ at 30 mV/s, and 7.8 F/cm$^3$ at 75 mV/s (see the details in **Supplementary Note 5)**. The experimental values we obtained at the corresponding operation rate are 12.1 F/cm$^3$ at 6 mV/s, 8.7 F/cm$^3$ at 30 mV/s, and 7.4 F/cm$^3$ at 75 mV/s (**Supplementary Fig. 9**). All these achieved experimental values are very close to the predicted pairing results. Meanwhile, we also monitored the actual potential window at varied operation rates and found they are also very close to the values intended. For example, when the working voltage of the as-fabricated supercapacitor cell is 1.6 V, the actual potential window recorded at the positive electrode is 0.560 V at 6 mV/s, 0.545 V at 30 mV/s, and 0.552 V at 75 mV/s. All are in good agreement with the intended working potential window of the positive electrode (0.55 V).

**Examining the key design parameters for cell-level optimisation**

As our pairings were conducted across the entire ranges of all the key targeted design parameters, the comprehensive data obtained allows us to systematically evaluate what design parameters could lead to the optimal cell performance and review how the traditional design

practice can be improved. Such an analysis also helps us to unveil the new engineering science insights for the EESD community that is difficult to gain through the conventional electrodes pairing practice. To achieve this, we calculated the volumetric capacitance of all the cells that can be numerically paired according to Eqs. 1-3 and presented the detailed results in the **Supplementary files of electrodes pairing** and some representative results in **Table 1**.

**Table 1.** A list of optimal volumetric capacitance values of supercapacitor cells ($C_{\text{v-cell\_t}}$) and the corresponding structural parameters of positive and negative electrodes in the examined range of structural parameters at selected operation rates of the cell ($\nu_{\text{\_cell}}$) and the thickness ($t$) of inactive components. The slit pore size and electrode thickness for the paired positive and negative electrodes that led to the optimal values are given as [$d_+$; $t_+$] and [$d_-$; $t_-$]. The results are from the cell with the inactive component of three thicknesses (0, 65, and 130 μm).

| $\nu_{\text{\_cell}}$ (mV/s) | $C_{\text{v-cell\_0}}$ [$d_+;t_+$ \|\| $d_-;t_-$] F/cm$^3$ [nm;μm\|\|nm;μm] | $C_{\text{v-cell\_65}}$ [$d_+;t_+$ \|\| $d_-;t_-$] F/cm$^3$ [nm;μm\|\|nm;μm] | $C_{\text{v-cell\_130}}$ [$d_+;t_+$ \|\| $d_-;t_-$] F/cm$^3$ [nm;μm\|\|nm;μm] |
|---|---|---|---|
| **6** | 22.0 [0.80;35\|\|0.81;14] | 12.4 [0.80;96.5\|\|0.80;31] | 9.8 [1.15;171\|\|0.80;43] |
| **30** | 19.7 [0.81;31\|\|0.88;11] | 9.1 [1.25;103\|\|0.80;22] | 6.9 [1.25;118\|\|0.80;24] |
| **75** | 17.0 [0.81;24\|\|1.37;11] | 7.8 [1.35;73\|\|0.80;15] | 5.5 [1.35;83\|\|0.80;16] |

Our results provide the opportunity to study the optimal design of supercapacitors under various operating conditions and quantitatively analyse the effect of the operation rates on the optimal design of supercapacitors. When the inactive component is not considered, which is often practiced in the laboratory-based research study, at a relatively low operation rate (6 mV/s) of the supercapacitor, the slit pore sizes of the two electrodes required to realize the maximal $C_{\text{v-cell}}$ are very close (0.80 nm and 0.81 nm, respectively). This is in agreement with the traditional design practice where the porous electrode materials with the same pore size are routinely used for both electrodes. However, at the higher charging rates, as generally required for the real-world use of supercapacitors[2], our data show that the slit pore sizes of the two electrodes required for the realisation of optimised $C_{\text{v-cell}}$ are rather different, a direct reflection of the asymmetry in the charging kinetics of the electrode materials under different polarization. In practice, this means that different porous carbon materials should be used for the paired

electrodes in the design of high-rate supercapacitors in contrast to what is traditionally practiced for electrical double layer-type supercapacitors.

When the inactive components of supercapacitors are taken into account, which is required for industrial applications, the structural parameters of electrodes to realize the highest C_(v-cell) are also found to be varied for different operation rates. For example, if an inactive component of 65 μm thickness is used, to achieve the optimal design of the supercapacitor cells at a charging rate of 6 mV/s, the slit pore size of positive and negative electrodes should be 0.80 nm (**Table 1**). When the supercapacitor cell is intended for optimal use at a charging rate of 75 mV/s, the paired slit pore size of positive and negative electrodes should be 1.35 and 0.80 nm, respectively. They are rather different from those of the cells optimised for optimal use at 6 and 30 mV/s. We also have conducted several control experiments to examine this trend. We fabricated the supercapacitors with the electrode parameters to be tailored to realize the optimal $C_{v-cell}$ at one charge rate and tested its performance at other operation rates. The resultant volumetric capacitance of the supercapacitor cell was indeed found to be lower than that of the optimal volumetric capacitance predicted at the tested operation rates (**Supplementary Table 3**). For example, when selecting the optimal structural parameters at 6 mV/s to design the supercapacitor cell working at 75 mV/s, the achieved volumetric capacitance of the supercapacitor cell is 4.3 F/cm$^3$, which is only 58.1% of the volumetric capacitance (7.4 F/cm$^3$) of the supercapacitor cell fabricated based on the optimal electrodes pairing at 75 mV/s.

Our results also offer a great opportunity to quantitatively examine how the dimension of the inactive components affects the volumetric performance of EESDs and optimal electrodes pairing. In the literature, the influence of inactive components on the device performance is often neglected, leading to much-inflated reporting performance data on their device fabricated based on the new electrode materials developed[2,56]. It is recommended that the real performance values of an EESD could be estimated by multiplying the inflated value with the volume/mass ratio of the active components in the entire device[2]. This recommendation is certainly valuable to help inexperienced researchers understand the true metrics for EESDs. However, our analysis reveals that the volumetric capacitance normalized by linearly scaling down an optimized $C_{v-cell}$ value may not be maximal anymore after $V_{inactive}$ is taken into account. For example, at the charge rate of 6 mV/s for the supercapacitor cell, without considering $V_{inactive}$, the optimal volumetric capacitance of the cell is 22.0 F/cm$^3$. Multiplying this value with the volume ratio of the active components in the entire device when the thickness of the inactive component is 65 μm, the calculated volumetric capacitance of the

device is 9.4 F/cm$^3$ at this charging rate, which is 24% lower than that of the maximal volumetric capacitance of the device that can be achieved with other pairing parameters at this operation rate (**Supplementary Table 4**). Such a discrepancy can be qualitatively explained due to the nonlinear relationship between $C_{\text{v-cell}}$ and the dimension of inactive components (Eq. 3). Meanwhile, at a given operation rate of the supercapacitor cell, with the thickness change of the inactive component, to achieve the optimal volumetric capacitance of resultant supercapacitor cells, there is also the pairing change for the structural parameters of positive and negative electrodes (**Table 1**). For example, at 6 mV/s of the supercapacitor cell, if the thickness of the inactive component is 65 μm, to achieve the optimal design of the supercapacitor cell, the slit pore size and thickness of the positive electrode is 0.80 nm and 96.5 μm, the corresponding slit pore size and thickness of the negative electrode is 0.8 nm and 30 μm. When the thickness of the inactive component increases to 130 μm, to achieve the optimal volumetric capacitance of the supercapacitor cell at this working rate, the slit pore size and thickness of positive electrode changes to 1.15 nm and 171 μm, the slit pore size and thickness of the negative electrode is 0.8 nm and 43 μm. These findings suggest that the role of inactive components should be examined for the future cell-level optimisation of EESDs from a holistic system engineering viewpoint.

Our results also present a tangible case to help properly understand the correlation of the performance of individual electrodes and supercapacitor cells, which is often confusing to inexperienced researchers in the fields of EESDs. As shown in **Fig. 1** and other reports[6,48,50], the performance of a supercapacitor electrode is dependent on its structural parameters (pore size, thickness) and charge rate. However, when paired electrodes into a real device, the cell-level performance is also related to the pairing of the structural parameters of positive and negative electrodes, the $C_{v+}$ and $C_{v-}$ may not necessarily be at their maximal values when the cell achieves the optimal volumetric capacitance (**Supplementary Table 5-7**). For example, when the inactive component of 65 μm thick is used, to achieve the optimal volumetric capacitance of the cell at the charge rate of 6 and 75 mV/s, respectively, the paired volumetric capacitance of positive and negative electrodes is 72 F/cm$^3$||119 F/cm$^3$ and 47 F/cm$^3$||120 F/cm$^3$, respectively, which is lower than that of the maximal values of $C_{v+}$ (89 F/cm$^3$) and $C_{v-}$ (123 F/cm$^3$).

## Discussion

To demonstrate the advantage of the data-driven approach over the traditional trial-and-error approach for the optimal design of supercapacitor, we have compared the results of ML-

assisted supercapacitors design and the general applied practices for the design of supercapacitors. For the most reported supercapacitor design strategy which the positive and negative active materials have the same pore structure, the researchers adjust the mass loading or thickness ratio of positive and negative electrodes experimentally to achieve the optimal design of the supercapacitors[7,15,25-26]. Compared to this generally used supercapacitor design strategy, our achieved supercapacitors based on the ML-assisted design method present larger cell capacitance and much higher optimal cell design efficiency (**Supplementary Table 8**). Meanwhile, compared with the traditional symmetric supercapacitor design, our ML-assisted designed supercapacitors also exhibit better performance, especially much higher working voltage (**Supplementary Table 3**, and **Supplementary Fig. 10-11**). Additionally, without the assistance of the ML method, we designed the supercapacitor cells following the same design principles only based on the experimental data. We were only able to achieve the supercapacitor design which works at the operation rate of 30 mV/s due to the requirement of the charge rate ratio of positive and negative electrodes. The resultant design results show that the optimal supercapacitor capacitance based on the experimental data is lower than that of the ML-assisted optimal designed supercapacitors (**Supplementary Table 9**). For example, when the inactive component of 130 μm thick is used, the optimal volumetric capacitance of the supercapacitor cell achieved only based on experimental data is 4.8 F/cm$^3$, which is 69% of the volumetric capacitance (6.9 F/cm$^3$) of the ML-assisted optimal designed supercapacitors.

We have also statistically analysed the data in the **Supplementary files of electrodes pairing**. We found that the volumetric capacitance distribution of the as-achieved supercapacitor cells is in a broad range and depends on the operation rate and thickness of inactive components (**Supplementary Figs. 12a-12c**). The probability for achieving the top 10% volumetric capacitance of the cell is less than 0.1% for all the cases we examined with the satisfaction of Eqs. 1-3 (**Supplementary Fig. 12d**). Interestingly, the results also show that there is an overlap of the volumetric capacitance of the resultant cells when charging the cells at different charging rates (**Supplementary Figs. 12a-12c**), further demonstrating the importance and necessity of the operation rate-dependent numerical pairing of positive and negative electrodes to achieve the cells with optimal volumetric capacitance. These results suggest the insurmountable challenge of using the traditional trial-and-error approach for the performance optimization of EESD

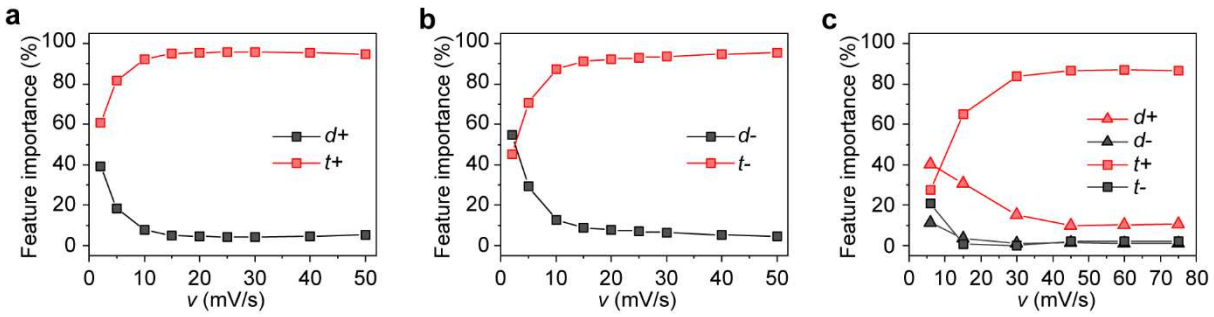


**Fig. 4 | Feature importance of the electrode structure parameters on the volumetric capacitance of individual electrodes and supercapacitor cells, respectively. a** and **b,** The feature importance score of electrode structure parameters on the volumetric capacitance of positive and negative electrodes, respectively. **c**, The feature importance score of electrode structure parameters on the volumetric capacitance of supercapacitor cell. The inactive component with a thickness of 65 μm was considered in the evaluation.

We have further applied a random forest regressor to quantitatively evaluate the weighting of each design parameter in the capacitive performance of individual electrodes and cells at a given condition. The results show that the importance level of each parameter on the volumetric capacitance of electrodes and cells, such as the slit pore size or the electrode thickness, is quite different and depends on the operation rate (**Fig. 4**). For instance, with the increase of the given operation rates, the importance weighting becomes higher for electrode thickness but lower for the slit pore size for both positive and negative electrodes (**Figs. 4a and 4b**). Interestingly, the importance score of electrode thickness for determining the volumetric capacitance of electrodes is always higher than that of the slit pore size of electrodes except for the negative electrode working at a low charge rate (2 mV/s). At a low operation rate (6 mV/s) for the supercapacitor cell, the most crucial electrode parameter in determining the volumetric capacitance of supercapacitor cell is the slit pore size of the positive electrode. When the charge rate is increased to 75 mV/s, the most influential parameter is changed to the thickness of the positive electrode (**Fig. 4c**). We also find that the structural parameters of the positive electrode always are more influential than that of the negative electrode for the volumetric capacitance of supercapacitor cells, indicating the predominant role of the positive electrode for the resultant supercapacitor cells. These results will be particularly valuable for guiding the priority level of design when the optimization of some parameters is prohibitive due to practical technical or cost restraints.

Given that many other EESDs such as batteries and hybrid capacitors are also involved with imbalanced charging kinetics between positive and negative electrodes and rate-dependent

performance, we hope that our findings revealed in this work could inspire researchers in other EESD fields to rethink the existing design practice and explore whether the domain knowledge-guided ML can be adopted to tackle these problems that are too difficult for the existing methods. Providing comprehensive data to reveal the remarkable effects of the specific testing conditions on the performance of an EESD at both the individual electrodes and cell levels and the complex relationships between them, this work highlights the great necessity of the previous call for the proper use of true performance metrics[2,4] and the need for a systems materials engineering approach for the broad field of EESDs[3]. We also hope that our finding that the best cell performance does not necessarily result from the best individual components suggests the great value of comprehensively reporting the research data including negative results.

## References


1 Crabtree, G., G. Rubloff, and E. Takeuchi. "Basic research needs for next generation electrical energy storage." Report of the Office of Basic Energy Sciences Workshop on Energy Storage. Washington, DC: *US Department of Energy Office of Science* **1**, (2017).

2 Gogotsi, Y. & Simon, P. Materials science. True performance metrics in electrochemical energy storage. *Science* **334**, 917-918 (2011).

3 Yang, P. & Tarascon, J. M. Towards systems materials engineering. *Nat. Mater.* **11**, 560-563 (2012).

4 Simon, P. & Gogotsi, Y. Perspectives for electrochemical capacitors and related devices. *Nat. Mater.* **19**, 1151-1163 (2020).

5 Zhao, J. & Burke, A. F. Electrochemical Capacitors: Performance Metrics and Evaluation by Testing and Analysis. *Adv. Energy Mater.* **11**, 2002192 (2021).

6 Yang, X., Cheng, C., Wang, Y., Qiu, L. & Li, D. Liquid-mediated dense integration of graphene materials for compact capacitive energy storage. *Science* **341**, 534-537 (2013).

7 Shao, Y. *et al.* Design and Mechanisms of Asymmetric Supercapacitors. *Chem. Rev.* **118**, 9233-9280 (2018).

8 Sun, G. *et al.* Capacitive matching of pore size and ion size in the negative and positive electrodes for supercapacitors. *Electrochim. Acta* **56**, 9248-9256 (2011).

9 Qiu, D. *et al.* Cucurbit[6]uril-Derived Sub-4 nm Pores-Dominated Hierarchical Porous Carbon for Supercapacitors: Operating Voltage Expansion and Pore Size Matching. *Small* **16**, e2002718 (2020).

10 Li, J. & Gao, F. Analysis of electrodes matching for asymmetric electrochemical capacitor. *J. Power Sources* **194**, 1184-1193 (2009).

11 Ike, I. S., Sigalas, I. & Iyuke, S. E. The influences of operating conditions and design configurations on the performance of symmetric electrochemical capacitors. *Phys. Chem. Chem. Phys.* **18**, 28626-28647 (2016).

12 Wu, T.-H., Hsu, C.-T., Hu, C.-C. & Hardwick, L. J. Important parameters affecting the cell voltage of aqueous electrical double-layer capacitors. *J. Power Sources* **242**, 289-298 (2013).

13 Van Aken, K. L., Beidaghi, M. & Gogotsi, Y. Formulation of ionic-liquid electrolyte to expand the voltage window of supercapacitors. *Angew. Chem. Int. Ed. Engl.* **54**, 4806-4809 (2015).

14 Peng, C., Zhang, S., Zhou, X. & Chen, G. Z. Unequalisation of electrode capacitances for enhanced energy capacity in asymmetrical supercapacitors. *Energy Environ. Sci.* **3**, 1499 (2010).

15 Li, H. *et al.* Quantifying the Volumetric Performance Metrics of Supercapacitors. *Adv. Energy Mater.* **9**, 1900079 (2019).

16 Anasori, B., Lukatskaya, M. R. & Gogotsi, Y. 2D metal carbides and nitrides (MXenes) for energy storage. *Nat. Rev. Mater.* **2**, 16098 (2017).

17 Sheberla, D. *et al.* Conductive MOF electrodes for stable supercapacitors with high areal capacitance. *Nat. Mater.* **16**, 220-224 (2017).

18 Zhong, C. *et al.* A review of electrolyte materials and compositions for electrochemical supercapacitors. *Chem. Soc. Rev.* **44**, 7484-7539 (2015).

19 Wang, X. *et al.* Electrode material–ionic liquid coupling for electrochemical energy storage. *Nat. Rev. Mater.* **5**, 787-808 (2020).

20 Pean, C. *et al.* Confinement, Desolvation, And Electrosorption Effects on the Diffusion of Ions in Nanoporous Carbon Electrodes. *J. Am. Chem. Soc.* **137**, 12627-12632 (2015).

21 Forse, A. C., Merlet, C., Griffin, J. M. & Grey, C. P. New Perspectives on the Charging Mechanisms of Supercapacitors. *J. Am. Chem. Soc.* **138**, 5731-5744 (2016).

22 Forse, Alexander C. *et al.* Direct observation of ion dynamics in supercapacitor electrodes using in situ diffusion NMR spectroscopy. *Nat. Energy* **2**, 16216 (2017).

23 Ye, J. *et al.* Charge Storage Mechanisms of Single-Layer Graphene in Ionic Liquid. *J. Am. Chem. Soc.* **141**, 16559-16563 (2019).

24 Xiao, J. *et al.* Electrolyte gating in graphene-based supercapacitors and its use for probing nanoconfined charging dynamics. *Nat. Nanotech.* **15**, 683-689 (2020).

25 Mistry, A., Franco, A. A., Cooper, S. J., Roberts, S. A. & Viswanathan, V. How Machine Learning Will Revolutionize Electrochemical Sciences. *ACS Energy Lett.* **6**, 1422-1431 (2021).

26 Lombardo, T. *et al.* Artificial Intelligence Applied to Battery Research: Hype or Reality? *Chem. Rev.* (2021).

27 Gao, T. & Lu, W. Machine learning toward advanced energy storage devices and systems. *iScience* **24**, 101936 (2021).

28 Chen, C. *et al.* A Critical Review of Machine Learning of Energy Materials. *Adv. Energy Mater.* **10**, 1903242 (2020).

29 Gu, G. H., Noh, J., Kim, I. & Jung, Y. Machine learning for renewable energy materials. *J. Mater. Chem. A* **7**, 17096-17117 (2019).

30 Min, K., Choi, B., Park, K. & Cho, E. Machine learning assisted optimization of electrochemical properties for Ni-rich cathode materials. *Sci. Rep.* **8**, 15778 (2018).

31 Bhowmik, A. *et al.* A perspective on inverse design of battery interphases using multi-scale modelling, experiments and generative deep learning. *Energy Storage Mater.* **21**, 446-456 (2019).

32 Cunha, R. P., Lombardo, T., Primo, E. N. & Franco, A. A. Artificial Intelligence Investigation of NMC Cathode Manufacturing Parameters Interdependencies. *Batteries & Supercaps* **3**, 60-67 (2019).

33 Turetskyy, A. *et al.* Toward Data-Driven Applications in Lithium-Ion Battery Cell Manufacturing. *Energy Technology* **8**, 1900136 (2019).

34 Dixit, M. B. *et al.* Synchrotron Imaging of Pore Formation in Li Metal Solid-State Batteries Aided by Machine Learning. *ACS Appl. Energy Mater.* **3**, 9534-9542 (2020).

35 Jiang, Z. *et al.* Machine-learning-revealed statistics of the particle-carbon/binder detachment in lithium-ion battery cathodes. *Nat. Commun.* **11**, 2310 (2020).

36 Severson, K. A. *et al.* Data-driven prediction of battery cycle life before capacity degradation. *Nat. Energy* **4**, 383-391 (2019).

37 Attia, P. M. *et al.* Closed-loop optimization of fast-charging protocols for batteries with machine learning. *Nature* **578**, 397-402 (2020).

38 Zhu, S. *et al.* Artificial neural network enabled capacitance prediction for carbon-based supercapacitors. *Mater. Lett.* **233**, 294-297 (2018).

39 Su, H. *et al.* Predicting the capacitance of carbon-based electric double layer capacitors by machine learning. *Nanoscale Advances* **1**, 2162-2166 (2019).

40 Zhou, M., Gallegos, A., Liu, K., Dai, S. & Wu, J. Insights from machine learning of carbon electrodes for electric double layer capacitors. *Carbon* **157** (2020).

41 Liu, P. *et al.* An emerging machine learning strategy for the assisted-design of high-performance supercapacitor materials by mining the relationship between capacitance and structural features of porous carbon. *J. Electroanalytical Chemistry* **899**, 115684 (2021).

42 Lukatskaya, M. R., Dunn, B. & Gogotsi, Y. Multidimensional materials and device architectures for future hybrid energy storage. *Nat. Commun.* **7**, 12647 (2016).

43 Conway, Brian E. Electrochemical supercapacitors: scientific fundamentals and technological applications. Springer Science & Business Media, 2013.

44 Jiang, G., Cheng, C., Li, D. & Liu, J. Z. Molecular dynamics simulations of the electric double layer capacitance of graphene electrodes in mono-valent aqueous electrolytes. *Nano Res.* **9**, 174-186 (2016).

45 Banda, H. *et al.* Ion Sieving Effects in Chemically Tuned Pillared Graphene Materials for Electrochemical Capacitors. *Chem. Mater.* **30**, 3040-3047 (2018).

46 Li, H. *et al.* Ultra-thick graphene bulk supercapacitor electrodes for compact energy storage. *Energy Environ. Sci.* **9**, 3135-3142 (2016).

47 Liu, L. *et al.* Evaluating the Role of Nanostructured Current Collectors in Energy Storage Capability of Supercapacitor Electrodes with Thick Electroactive Materials Layers. *Adv. Funct. Mater.* **28**, 1705107 (2017).

48 Chmiola, J. Anomalous Increase in Carbon Capacitance at Pore Sizes Less Than 1 Nanometer. *Science* **313**, 1760-1763 (2006).

49 Kondrat, S., Pérez, C. R., Presser, V., Gogotsi, Y. & Kornyshev, A. A. Effect of pore size and its dispersity on the energy storage in nanoporous supercapacitors. *Energy Environ. Sci.* **5**, 6474 (2012).

50 Liu, C. *et al.* Toward Superior Capacitive Energy Storage: Recent Advances in Pore Engineering for Dense Electrodes. *Adv. Mater.* **30**, e1705713 (2018).

51 Yu, M., Lu, Y., Zheng, H. & Lu, X. New Insights into the Operating Voltage of Aqueous Supercapacitors. *Chemistry : A European Journal* **24**, 3639-3649 (2018).

52 Khomenko, V., Raymundo-Piñero, E. & Béguin, F. A new type of high energy asymmetric capacitor with nanoporous carbon electrodes in aqueous electrolyte. *J. Power Sources* **195**, 4234-4241 (2010).

53 Kondrat, S., Wu, P., Qiao, R. & Kornyshev, A. A. Accelerating charging dynamics in subnanometre pores. *Nat. Mater.* **13**, 387-393 (2014).

54 Salanne, M. *et al.* Efficient storage mechanisms for building better supercapacitors. *Nat. Energy* **1**, 16070 (2016).

55 Childs, C. M. & Washburn, N. R. Embedding domain knowledge for machine learning of complex material systems. *MRS Commun.* **9**, 806-820 (2019).

56 Noori, A., El-Kady, M. F., Rahmanifar, M. S., Kaner, R. B. & Mousavi, M. F. Towards establishing standard performance metrics for batteries, supercapacitors and beyond. *Chem. Soc. Rev.* **48**, 1272-1341 (2019).



**Acknowledgements**

We would like to acknowledge the financial support from the Australia Research Council (DP180102890 and FL180100029) and The University of Melbourne. The authors thank Dr. Hualin Zhan for an initial discussion on the machine learning method.

**Author contributions**

L.B.Q. conceived, designed and carried out the experiments and analysed the experimental results under the guidance of D.L. and J.Z.L. D. L. J. Z. L. and L.B.Q. formulated the concept of applying machine learning models to assist the electrodes pairing. L.B.Q., P.Y.W. and B. M designed and carried out the machine learning modelling and analysed the machine learning model results. L.B.Q and P.Y.W. conducted the electrodes pairing and analysed the electrodes pairing results. All authors participate the discussion of the manuscript writing. L.B.Q. J.Z.L and D.L. wrote the manuscript with contributions from all the other authors.

**Competing interests**

The authors declare no competing interests.

**Data availability**

The data that support the findings of this study are available from the corresponding author upon reasonable request.

**Additional information**

Supplementary information is available in the online version of the paper. Reprints and permission information is available online at www.nature.com/reprints. Correspondence and requests for materials should be addressed to D.L. and J.Z.L.

# Supplementary Files

This is a list of supplementary files associated with this preprint. Click to download.

- SINC.pdf
- Supplementalfilesofcodes.zip
- Supplementalfilesofelectrodespairing.zip
- Supplementalfilesofhyperparameter.zip